

## Particle swarm optimization of TMD by non-stationary base excitation during earthquake

A. Y. T. Leung<sup>\*,†</sup>, Haijun Zhang, C. C. Cheng and Y. Y. Lee

*Department of Building and Construction, City University of Hong Kong, Hong Kong*

### SUMMARY

There are many traditional methods to find the optimum parameters of a tuned mass damper (TMD) subject to stationary base excitations. It is very difficult to obtain the optimum parameters of a TMD subject to non-stationary base excitations using these traditional optimization techniques. In this paper, by applying particle swarm optimization (PSO) algorithm as a novel evolutionary algorithm, the optimum parameters including the optimum mass ratio, damper damping and tuning frequency of the TMD system attached to a viscously damped single-degree-of-freedom main system subject to non-stationary excitation can be obtained when taking either the displacement or the acceleration mean square response, as well as their combination, as the cost function. For simplicity of presentation, the non-stationary excitation is modeled by an evolutionary stationary process in the paper. By means of three numerical examples for different types of non-stationary ground acceleration models, the results indicate that PSO can be used to find the optimum mass ratio, damper damping and tuning frequency of the non-stationary TMD system, and it is quite easy to be programmed for practical engineering applications. Copyright © 2008 John Wiley & Sons, Ltd.

Received 9 August 2007; Revised 12 February 2008; Accepted 20 February 2008

**KEY WORDS:** TMD; optimum parameters; damped system; PSO; non-stationary excitation; Runge–Kutta; numerical integration; mean square response

### INTRODUCTION

Tuned mass dampers (TMDs) are among the oldest passive structural vibration control devices [1]. The concept of vibration control using a mass damper can be dated back to the year 1909, when

---

\*Correspondence to: A. Y. T. Leung, Department of Building and Construction, City University of Hong Kong, Hong Kong.

†E-mail: andrew.leung@cityu.edu.hk

Contract/grant sponsor: Research Grant Council of Hong Kong; contract/grant number: CERG#115706

Frahm invented a vibration control device called a dynamic vibration absorber. There has been a resurgence of interest in the study of TMD in recent years. A great number of newer tall buildings are now equipped with various versions of TMD system for vibration attenuation under wind and moderate earthquakes. A summary of these applications including the Taipei 101 Tower can be found in Lee *et al.* [2]. Thus, the understanding of the TMD behavior and its design parameters becomes important. The mechanism of a TMD system consists of a mass, a spring, and a dashpot that is attached to a main structure whose dynamic response is to be attenuated. The structure motion is essentially controlled during the excitation by appending the structure with a TMD system that absorbs most of the input energy so that only a part of this energy is transferred to the main structural system. One of the most important design issues is the parameter optimization. The parameters to be optimally designed include the mass, damping and stiffness of the TMD system.

As for the issue of the stationary random excitations applying to the main system, optimum TMD parameters had been widely studied by many researchers. Den Hartog [3] and Brock [4] gave an explicit solution for determining optimum TMD parameters for undamped main system subjected to harmonic external force over a broad band of excitation frequency. Warburton and Ayorinde [5, 6] successfully proved the possibility of and accuracy in idealizing a multi-degree-of-freedom main system as a single-degree-of-freedom (SDOF) system by solving numerous elastic structures such as plates, beams and shells equipped with a TMD, assuming that the natural frequencies are well separated. At the same time, Warburton [7, 8] derived the sample expressions for optimum absorber parameters for undamped and damped one-degree-of-freedom main systems under harmonic and white noise random excitations with force and base acceleration as input and for minimization of various response parameters in different cases. In addition, classical and graphical solutions were also obtained for finding the optimum parameters of untuned vibration absorber by Bapat and Kumaraswamy [9] and Thompson [10], respectively. Tsai and Lin [11, 12] proposed a numerical iteration searching technique to find the optimum damping and tuning frequency ratio of the TMD system for minimizing the steady-state response of support-excited and damped systems and also provided explicit formulae for the resulting optimum absorber parameters for force-excited and viscously damped system by using curve-fitting method. Jangid [13] and Bakre and Jangid [14, 15] employed the same numerical iteration searching technique for optimizing single and multiple TMDs for base-excited undamped and damped systems, respectively, and developed explicit expressions after several trials using the curve-fitting scheme.

However, in earthquakes, excitations are often modeled as non-stationary random processes. Unfortunately, compared with the cases of stationary excitations, due to the complexity of the response integration, it is difficult to obtain the explicit expressions of the optimum TMD parameters and to analyze the response characteristics of the main system equipped with a TMD. It is almost impossible to obtain the optimum TMD parameters by using the similar numerical iteration technique or conventional mathematical methods. Jangid [16] applied the energy content theory of the modulating function to investigate the non-stationary response of an SDOF system subject to non-stationary earthquake motion for different shapes of modulating functions. Closed-form expressions for the time-varying frequency response function were derived for different shapes of the modulating functions. Li [17] proposed a numerical calculation method for the mean square evolutionary random seismic response of building structures with a TMD by using the Runge–Kutta direct integration method and modal analysis. He summarized the resulting TMD parameters by experiences after a great number of

computing trials. To the best of our knowledge, the optimum TMD parameters of a damped main system subject to non-stationary random excitations have not been obtained by optimization methods.

Recently, a novel evolutionary technique, namely particle swarm optimization (PSO), had been proposed [18–20]. The development was based on the observations of the social behavior of animals, such as bird flocking, fish schooling and swarm theory. PSO is initialized with a population of random solutions. Each individual is assigned with a randomized velocity according to the flying experiences of itself and its companions. The individuals, called particles, are then flown through hyperspace. Compared with other evolutionary algorithms, such as the genetic algorithm (GA) and the ant colony optimization (ACO) algorithm, PSO has some attractive characteristics. It has memory. The knowledge of good solutions is retained by all particles, whereas in GA, previous knowledge of the problem is destroyed once the population changes. At the same time, ACO is not suitable for solving continuous optimization problems. In PSO, there is a constructive cooperation between particles that share information. Owing to the simple concept, easy implementation and quick convergence, nowadays, PSO has gained much attention and a wide variety of applications in a variety of fields [21–25]. In this paper, we will use PSO to obtain the optimum mass, damping and tuning frequency ratio of the TMD system when the main system is excited by non-stationary random ground acceleration for the minimization of displacement mean square response. As displacement is related to acceleration by the frequency, acceleration can also be reduced. For simplicity of presentation, the non-stationary excitation is modeled by an evolutionary stationary process in the paper. Three numerical examples for different non-stationary ground acceleration models are given to demonstrate the efficiency and availability of the proposed method, and it is quite convenient for practical engineering application.

The remaining contents of this paper are organized as follows. The structural mathematical model and the optimization problem are first represented. The PSO algorithm is described in detail and the optimization procedure of optimum TMD parameters for damped main system under non-stationary random ground acceleration is summarized. Three numerical examples for different non-stationary random ground acceleration models are then given and the paper ends with some conclusions and future work propositions.

## STRUCTURAL MODEL AND STATEMENT OF OPTIMIZATION PROBLEM

The schematic diagram of a main system equipped with a TMD and excited by the non-stationary random ground acceleration is shown in Figure 1. The main system is characterized by the mass  $m_s$ , the stiffness  $k_s$  and the damping  $c_s$ . The natural frequency and viscous damping ratio of the main system are  $\omega_s = \sqrt{k_s/m_s}$  and  $\zeta_s = c_s/2\sqrt{k_s m_s}$ , respectively. Similar to the main system, the TMD consists of the mass  $m_T$ , the stiffness  $k_T$  and the damping  $c_T$ . Let  $\omega_T = \sqrt{k_T/m_T}$  and  $\zeta_T = c_T/2\sqrt{k_T m_T}$  denote the natural frequency and damping ratio of the TMD, respectively. On the other hand, the mass and tuning frequency ratio of the TMD are defined as  $\mu = m_T/m_s$  and  $f = \omega_T/\omega_s$ .

In the present study, the ground acceleration applied to the base of the main system,  $\ddot{u}_g$ , is a non-stationary random process, and the main system equipped with a TMD is modeled as an SDOF system.

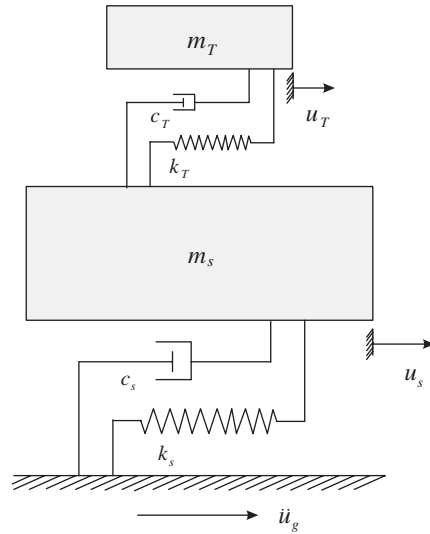


Figure 1. A single-degree-of-freedom main system equipped with a TMD.

### Mean square response

The equation of motion for the whole system excited by the ground acceleration,  $\ddot{u}_g$ , applied to the main system can be expressed as follows:

$$\begin{bmatrix} m_s & 0 \\ 0 & m_T \end{bmatrix} \begin{Bmatrix} \ddot{u}_s \\ \ddot{u}_T \end{Bmatrix} + \begin{bmatrix} c_s + c_T & -c_T \\ -c_T & c_T \end{bmatrix} \begin{Bmatrix} \dot{u}_s \\ \dot{u}_T \end{Bmatrix} + \begin{bmatrix} k_s + k_T & -k_T \\ -k_T & k_T \end{bmatrix} \begin{Bmatrix} u_s \\ u_T \end{Bmatrix} = - \begin{Bmatrix} m_s \\ m_T \end{Bmatrix} \ddot{u}_g \quad (1)$$

where  $u_s$  is the displacement of the main system relative to the ground,  $u_T$  is that of the TMD relative to the ground and  $\ddot{u}_g$  is the non-stationary random ground acceleration exerting on the main system.

Denote the state vector by  $Z = [u_s \ u_T \ \dot{u}_s \ \dot{u}_T]^T$ , then Equation (1) can be transformed into

$$\dot{Z} = AZ + B\ddot{u}_g \quad (2)$$

where

$$A = \begin{bmatrix} 0 & 0 & 1 & 0 \\ 0 & 0 & 0 & 1 \\ -(k_s + k_T)/m_s & k_T/m_s & -(c_s + c_T)/m_s & c_T/m_s \\ k_T/m_T & -k_T/m_T & c_T/m_T & -c_T/m_T \end{bmatrix}, \quad B = [0 \ 0 \ -1 \ -1]^T$$

At the same time, the autocorrelation function of the ground acceleration can be expressed as [26, 27]

$$C_{\ddot{u}_g \ddot{u}_g}(\tau, t) = E[\ddot{u}_g(\tau)\ddot{u}_g(t)] = \int_{-\infty}^{\infty} \lambda(\omega, \tau)\lambda(\omega, t)e^{j\omega(t-\tau)} S(\omega) d\omega \quad (3)$$

When the non-stationary excitation is modeled by an evolutionary stationary process, the power spectral density of the non-stationary random ground acceleration is given by

$$S_{\ddot{u}_g}(\omega, t) = |\lambda(\omega, t)|^2 S(\omega) \tag{4}$$

where  $\lambda(\omega, t)$  is a deterministic evolutionary function of  $t$  and  $\omega$ , and  $S(\omega)$  is the power spectral density of the stationary random process.

Then, the corresponding mean square response matrix from Equation (2) can be expressed as

$$E[Z(t)Z^T(t)] = E \left\{ \begin{bmatrix} u_s^2 & u_s u_T & u_s \dot{u}_s & u_s \dot{u}_T \\ u_T u_s & u_T^2 & u_T \dot{u}_s & u_T \dot{u}_T \\ \dot{u}_s u_s & \dot{u}_s u_T & \dot{u}_s^2 & \dot{u}_s \dot{u}_T \\ \dot{u}_T u_s & \dot{u}_T u_T & \dot{u}_T \dot{u}_s & \dot{u}_T^2 \end{bmatrix} \right\} \\ = \int_{-\infty}^{\infty} H(\omega, t) S(\omega) H(\omega, t)^* d\omega = 2 \int_0^{\infty} H(\omega, t) S(\omega) H(\omega, t)^* d\omega \tag{5}$$

where  $H(\omega, t)$  is the evolutionary frequency response function, and it is the transient response of the main system subjected to the deterministic excitation,  $\lambda(\omega, t)e^{-j\omega t}$ , as described in Equation (4) under a zero initial condition [26].  $A^*$  denotes conjugate transposition.

Usually, it is extremely difficult to obtain the frequency response function  $H(\omega, t)$  in closed form. However, it is sufficient to obtain the specified solution to Equation (2) using numerical methods. Then, substituting  $\lambda(\omega, t)e^{-j\omega t}$  for the non-stationary random excitation  $\ddot{u}_g$  into Equation (2), we can obtain

$$\dot{H}(\omega, t) = AH(\omega, t) + B\lambda(\omega, t)e^{-j\omega t} \tag{6}$$

Equation (6) is a set of first-order constant differential equations in time series  $t$ , which can be solved using the fourth-order Runge–Kutta integration method [17].

Thus, the displacement mean square response and the velocity mean square response of the main system can be solved directly from Equation (5), i.e.

$$E[u_s^2(t)] = E[M(1, 1)] \tag{7}$$

$$E[\dot{u}_s^2(t)] = E[M(3, 3)] \tag{8}$$

where

$$M = \begin{bmatrix} u_s^2 & u_s u_T & u_s \dot{u}_s & u_s \dot{u}_T \\ u_T u_s & u_T^2 & u_T \dot{u}_s & u_T \dot{u}_T \\ \dot{u}_s u_s & \dot{u}_s u_T & \dot{u}_s^2 & \dot{u}_s \dot{u}_T \\ \dot{u}_T u_s & \dot{u}_T u_T & \dot{u}_T \dot{u}_s & \dot{u}_T^2 \end{bmatrix}$$

and  $M(i, j)$  ( $i, j = 1, \dots, 4$ ) is the  $(i, j)$ th element of matrix  $M$ .

In addition, from Equation (5), we can obtain approximately

$$E[\ddot{Z}(t)\ddot{Z}^T(t)] = \int_{-\infty}^{\infty} \omega^4 H(\omega, t) S(\omega) H(\omega, t)^* d\omega = 2 \int_0^{\infty} \omega^4 H(\omega, t) S(\omega) H(\omega, t)^* d\omega \tag{9}$$

The acceleration mean square response of the main system will approximately be

$$E[\ddot{u}_s^2(t)] = E[M_a(1, 1)] \quad (10)$$

where

$$M_a = \begin{bmatrix} \ddot{u}_s^2 & \ddot{u}_s \ddot{u}_T & \ddot{u}_s \ddot{u}_s & \ddot{u}_s \ddot{u}_T \\ \ddot{u}_T \ddot{u}_s & \ddot{u}_T^2 & \ddot{u}_T \ddot{u}_s & \ddot{u}_T \ddot{u}_T \\ \ddot{u}_s \ddot{u}_s & \ddot{u}_s \ddot{u}_T & \ddot{u}_s^2 & \ddot{u}_s \ddot{u}_T \\ \ddot{u}_T \ddot{u}_s & \ddot{u}_T \ddot{u}_T & \ddot{u}_T \ddot{u}_s & \ddot{u}_T^2 \end{bmatrix}$$

and  $M(i, j)$  ( $i, j = 1, \dots, 4$ ) is the  $(i, j)$ th element of matrix  $M_a$ .

#### *Optimization problem of TMD under non-stationary random ground acceleration*

The optimized parameters of the TMD system consist of the mass, the damping and the stiffness. For the purpose of analysis and computation convenience, it is generally transferred to optimizing the mass, damping and tuning frequency ratio of the TMD system. Thus, the mass  $m_T$ , the damping  $c_T$  and the stiffness  $k_T$  of TMD can be obtained from

$$m_T = \mu m_s \quad (11)$$

$$c_T = 2\mu \xi_T f \sqrt{k_s m_s} \quad (12)$$

$$k_T = \mu f^2 k_s \quad (13)$$

Let  $N = E[u_s^2(t)]$  represent the displacement mean square response function of the main system about the time series  $t$ , the mass ratio  $\mu$ , the damping  $\xi_T$  and the tuning frequency ratio  $f$  of TMD. Then, the optimization problem of TMD can be expressed as

$$\begin{aligned} N^{\text{opt}} &= \min_{\mu, \xi_T, f} \max_t N(t, \mu, \xi_T, f) \\ &= \min_{\mu, \xi_T, f} \max_t E[u_s^2(t)] \end{aligned} \quad (14)$$

subject to  $\mu > 0$ ,  $\xi_T > 0$ ,  $f > 0$ .

In addition, for a specified mass ratio  $\mu = \mu_0$ , Equation (14) can be changed into

$$\begin{aligned} N^{\text{opt}} &= \min_{\xi_T, f} \max_t N(t, \mu_0, \xi_T, f) \\ &= \min_{\xi_T, f} \max_t E[u_s^2(t)] \end{aligned} \quad (15)$$

One can choose displacement or acceleration as cost function. In fact most authors use displacement as the cost function including Reference [2] and some others in the list of references. For a fixed frequency, the acceleration is almost proportional to the displacement. From our examples below, both displacement and acceleration are reduced by about 50% at optimal parameters.

## PARAMETERS OPTIMIZATION BASED ON PSO

*PSO algorithm*

PSO is an evolutionary computation technique through individual improvement in addition to population cooperation and competition. PSO is based on the simulation of simplified social models, such as bird flocking, fish schooling and the swarming theory. In PSO, multiple candidate solutions coexist and collaborate simultaneously. Each solution, called a 'particle,' flies in the exploration space of the optimization problem searching the optimal position to land. A particle, as time passes through its quest, adapts to adjust its position according to its own 'experience' as well as the experiences of neighboring particles. With tracking and memorizing the best position encountered, particles' experiences are accumulated as exploration proceeds. Thus, PSO possesses memory, i.e. every particle remembers the best position it reached in the past. At the same time, PSO combines the local search scheme through self-experience with the global search scheme through neighboring experience so that the best solution is obtained at the end. Therefore, PSO is substantially of a heuristic and parallel search technique due to a group of particles' exploration.

A particle status in the search space is characterized by two factors: position and velocity. The position and the velocity of the  $i$ th particle in the  $d$ -dimensional search space can be represented as  $X_i = (x_{i,1}, x_{i,2}, \dots, x_{i,d})$  and  $V_i = (v_{i,1}, v_{i,2}, \dots, v_{i,d})$ , respectively. The  $i$ th particle has its own best position  $P_i = (p_{i,1}, p_{i,2}, \dots, p_{i,d})$ , corresponding to the individual best objective value obtained so far at time  $\tau$ . The global best particle is denoted as  $g$ , which represents the best position found so far at time  $\tau$  in the whole swarm. The new velocity of each particle is given by

$$v_{i,j}(\tau+1) = wv_{i,j}(\tau) + c_1r_1[p_{i,j} - x_{i,j}(\tau)] + c_2r_2[g_j - x_{i,j}(\tau)], \quad j = 1, 2, \dots, d \quad (16)$$

where  $c_1$  and  $c_2$  are constants called the acceleration coefficients, usually  $c_1 = c_2 = 2$ ;  $r_1$  and  $r_2$  are two independent random numbers uniformly distributed in the range  $[0, 1]$ ;  $w$  is called the inertia factor, which is often in the range  $[0.1, 0.9]$ , and many previous studies show that if  $w$  declines linearly along with the exploration proceeding, it will improve the convergence performance greatly, and the updated equation is given by

$$w = w_{\max} - n_i \times \frac{(w_{\max} - w_{\min})}{n_{\max}} \quad (17)$$

where  $w_{\max}$  and  $w_{\min}$  are called the maximum and minimum weights, respectively,  $n_i$  is the current generation number and  $n_{\max}$  is the maximum number of generations.

The position of each particle is then updated in each generation according to the following equation:

$$x_{i,j}(\tau+1) = x_{i,j}(\tau) + v_{i,j}(\tau+1), \quad j = 1, 2, \dots, d \quad (18)$$

PSO is usually based on real encoding, and its structure is relatively simple due to the lack of cross and mutation as a result of higher running speed. In PSO, Equation (16) is applied to calculate the new velocity according to its previous velocity and to the distance of its current position from both its own best historical position and its neighbors' best position. Generally, the value of each component in  $V_i$  can be clamped to the range  $[v_{\min}, v_{\max}]$  to control the excessive roaming of particles outside the search space. Then, the particle flies towards a new position

according to Equation (16). This process is repeated until the maximum number of generations is reached.

#### *Optimum parameters of non-stationary TMD using PSO*

Based on PSO, a method to find the optimum parameters of non-stationary TMD is proposed. Here, the position vector and the objective value of each particle in PSO correspond to the parameters of TMD, i.e. the mass ratio  $\mu$ , the damping  $\xi_T$  and the tuning frequency ratio  $f$ , and the displacement mean square response of the main system, respectively. We use the numerical method presented by Reference [17] to evaluate the fitness of particles. To obtain the optimum parameters of non-stationary TMD, the procedure of PSO to optimize TMD parameters is summarized in detail as follows:

*Step 1:* Initialize the population of particles with random positions and velocities, where each particle  $X_i$  contains  $d(d=3)$  components.

*Step 2:* Evaluate the objective values of all particles.

*Step 2.1:* Form state matrices  $A$  and  $B$ .

*Step 2.2:* Set the maximum natural frequency  $\omega_{\max}$  and time series  $t_{\max}$ . Let time series  $t=0$ .

*Step 2.3:* Let natural frequency  $\omega=0$ ; set the initial value of the frequency response function  $H(\omega, t)$ ,  $H_0=0$ ; define  $E_s=0$ .

*Step 2.4:* Calculate the frequency response function  $H(\omega, t)$  by using the fourth-order Runge–Kutta integration method from Equation (6).

*Step 2.5:* Let  $\bar{H}_0 = H(\omega, t)$  and  $E_s = E_s + H(\omega, t)S(\omega)H(\omega, t)^*$ .

*Step 2.6:* Set  $\omega = \omega + \Delta\omega$  ( $\Delta\omega$  is the integration step size of natural frequency). If  $\omega < \omega_{\max}$ , go to Step 2.4; otherwise, go to Step 2.7.

*Step 2.7:* Calculate the response matrix  $E[Z(t)Z^T(t)] = 2E_s\Delta\omega$ , obtain the displacement mean square response of the main system  $E[u_s^2(t)]$  according to Equation (7) and reserve the current value of  $E[u_s^2(t)]$ .

*Step 2.8:* Set  $H_0 = \bar{H}_0$  and  $t = t + \Delta t$  ( $\Delta t$  is the integration step size of time series).

*Step 2.9:* If  $t \leq t_{\max}$ , go to Step 2.3; otherwise, use the queuing algorithm to find the maximum value of the displacement mean square response in the range of  $[0, t_{\max}]$ , then go to Step 3.

*Step 3:* Let each particle's own best position and its objective value be equal to its current position and objective value, and let the global best particle and its objective value be equal to the position and objective value of the best initial particle.

*Step 4:* Update the velocity and position of each particle according to Equations (16), (17) and (18).

*Step 5:* Evaluate the objective values of all particles, i.e. repeat Steps 2.1–2.9.

*Step 6:* For each particle, one compares its current objective value with the objective value of its own best position. If the current value is better, then update its own best position and its objective value with the current position and objective value.

*Step 7:* Determine the best particle of the current swarm according to the best objective value. If the objective value is better than the objective value of the global best position, then update the global best position and its objective value with the position and objective value of the current best particle.

*Step 8:* If the number of current generations  $n_i$  is smaller than the number of maximum generations  $n_{\max}$ , go to Step 4; otherwise, go to Step 9.

*Step 9:* Output the global best position and its objective value, and end the procedure.



NUMERICAL EXAMPLES

In order to demonstrate the efficiency of the proposed method to obtain the optimum parameters of non-stationary TMD, three different typical forms of the evolutionary power spectrum cited from Reference [26] are considered here, each of them can simulate the behavioral characteristics of actual earthquakes.

For the main system, suppose that the mass  $m_s = 1.0 \times 10^6$  kg, the stiffness  $k_s = 2.5 \times 10^7$  N/m and the damping  $c_s = 0.1\sqrt{k_s m_s}$  N s/m. The natural frequency is 5 rad/s, which is about 0.8 Hz. At the same time, the important parameters in the optimization programs are given as follows:  $n_{\max} = 50$  (maximum generations),  $N_p = 20$  (population size),  $w_{\max} = 0.9$ ,  $w_{\min} = 0.1$ ,  $\omega_{\max} = 200$  rad/s,  $\Delta\omega = 0.1$ ,  $t_{\max} = 15$  s,  $\Delta t = 0.1$ .

Power spectrum I

The evolutionary power spectrum is to simulate the behavior of the N-S component of the December 30, 1934 EI Centro earthquake, which is the product of the well-known Kanai-Tajimi spectrum for stationary random processes multiplied by an envelope function, and the evolutionary spectrum is expressed as

$$S_{\ddot{u}_g}(\omega, t) = |\lambda(\omega, t)|^2 S_0 \tag{19}$$

$$\lambda(\omega, t) = \frac{e^{-at} - e^{-bt}}{\max[e^{-at} - e^{-bt}]} \left\{ \frac{\omega_g^4 + 4\xi_g^2 \omega_g^2 \omega^2}{(\omega^2 - \omega_g^2)^2 + 4\xi_g^2 \omega_g^2 \omega^2} \right\}^{1/2} \tag{20}$$

where  $a = 0.25 \text{ s}^{-1}$ ;  $b = 0.50 \text{ s}^{-1}$ ;  $\xi_g = 0.25$ ;  $\omega_g = 15.0 \text{ rad/s}$ ;  $S_0 = 2.0 \text{ cm}^2/\text{s}^3$ .

According to the procedures mentioned in the last section, PSO is applied to optimize the TMD parameters for the main system. After several numerical simulations, we discover that the optimum response quantity  $N^{\text{opt}}$  decreases as the mass ratio  $\mu$  increases; thus, given to engineering applications, we optimize only the damping  $\xi_T$  and tuning frequency ratio  $f$  of TMD for a specified mass ratio  $\mu$ . The optimum parameters, the displacement mean square response quantities for a specified mass ratio  $\mu$  using PSO, are given in Table I. The optimum damping and tuning frequency of TMD for the main system are plotted in Figures 2 and 3 as functions of mass ratio. From Figure 2, it is seen that the optimum damping  $\xi_T^{\text{opt}}$  increases as the mass ratio  $\mu$  increases. From Figure 3, it is observed that the optimum tuning frequency  $f^{\text{opt}}$  decreases almost linearly with the increase in the mass ratio  $\mu$ .

To investigate the influence of the system mass ratio on the effectiveness of TMD, the variations of the displacement mean square responses and the corresponding velocity mean square responses

Table I. Optimum TMD parameters for the main system under non-stationary random ground acceleration with power spectrum I based on PSO for a specified mass ratio using displacement as the cost function.

$\mu$	0.01	0.02	0.03	0.04	0.05	0.06	0.07	0.08	0.09	0.1
$\xi_T^{\text{opt}}$	0.0000	0.0299	0.0501	0.0680	0.0870	0.1028	0.1148	0.1248	0.1510	0.1617
$f^{\text{opt}}$	0.8966	0.8685	0.8432	0.8216	0.8031	0.7853	0.7672	0.7494	0.7392	0.7241
$N^{\text{opt}} (\text{cm}^2)$	2.4486	2.1914	2.0363	1.9266	1.8456	1.7811	1.7293	1.6877	1.6520	1.6190

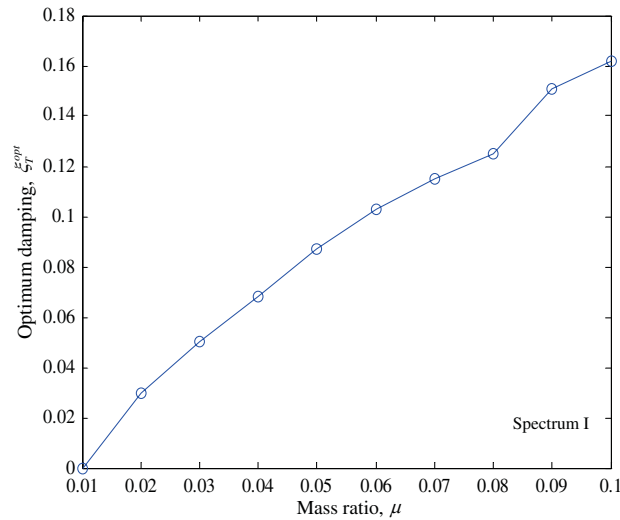


Figure 2. Optimum damping of a TMD for evolutionary spectrum I.

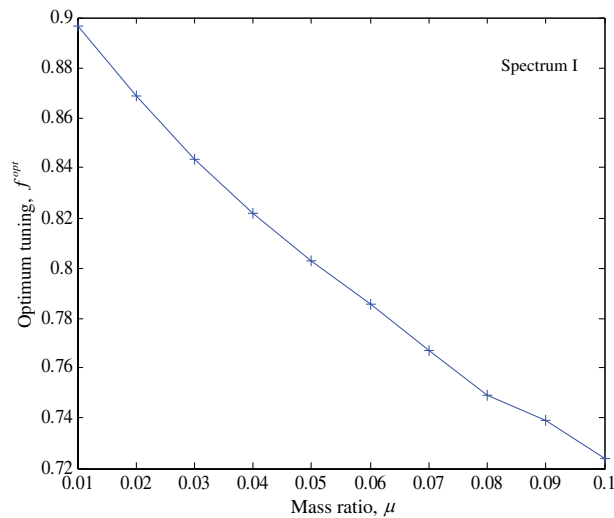


Figure 3. Optimum tuning frequency of a TMD for evolutionary spectrum I.

for different specified mass ratios  $\mu$  are plotted in Figures 4 and 5, respectively, which indicates that the system maximum responses further reduce with the increase in the mass of the optimum TMD. When the main system is not equipped with a TMD, then the mass ratio  $\mu=0$ . For the mass ratio  $\mu=0.1$ , compared with the case of the main system without a TMD, the maximum displacement mean square response  $E[u_s^2]$  and the maximum velocity mean square response  $E[\dot{u}_s^2]$  of the main reduce by decline 50.42 and 48.56%, respectively. The maximum acceleration mean square response  $E[\ddot{u}_s^2]$  is also reduced by 47.4% as shown in Figure 6.

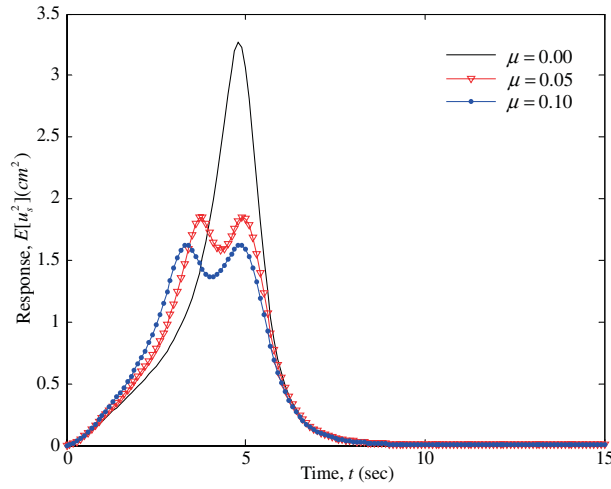


Figure 4. Optimum displacement mean square responses.

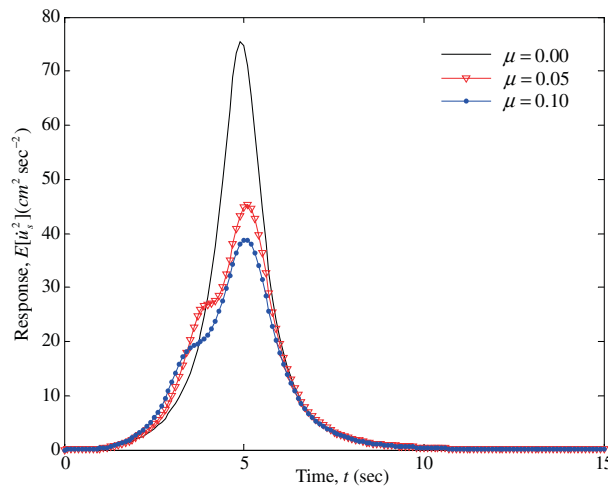


Figure 5. Corresponding velocity mean square responses.

One can use acceleration as the cost function

$$N^{opt} = \min_{\xi_T, f} \max_t E[\ddot{u}_s^2(t)]$$

for a PSO optimization. The results are tabulated in Table II and the displacement, velocity and acceleration mean square responses are shown in Figures 7–9, respectively. One can also use the

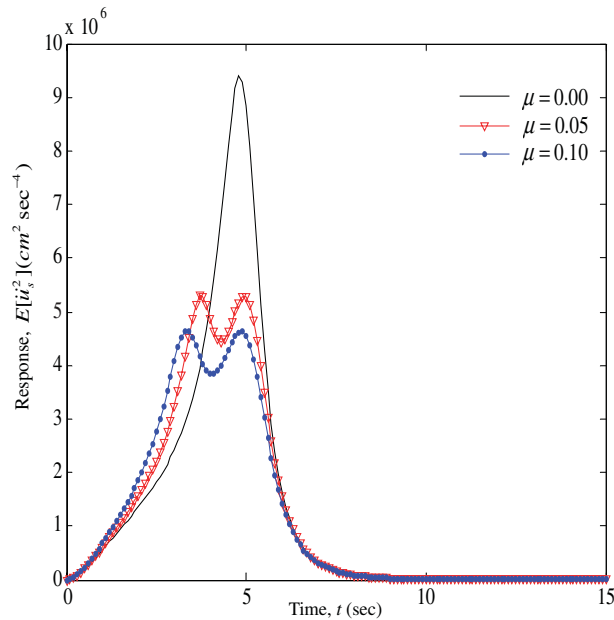


Figure 6. Corresponding acceleration mean square responses.

Table II. Optimum TMD parameters for the main system under non-stationary random ground acceleration with power spectrum I based on PSO for a specified mass ratio using acceleration as the cost function.

$\mu$	0.01	0.05	0.1
$\zeta_T^{\text{opt}}$	0.0000	0.0856	0.1600
$f^{\text{opt}}$	0.8956	0.8016	0.7231
$N^{\text{opt}}$ ( $\text{cm}^2/\text{s}^4$ )	$7.0309 \times 1.0\text{e}6$	$5.2893 \times 1.0\text{e}6$	$4.6320 \times 1.0\text{e}6$

combination of means square responses of displacement, velocity (stroke) and acceleration as the cost function

$$N^{\text{opt}} = \min_{\zeta_T, f} \max_t \{ E[u_s^2(t)]/u_m^2 + E[\dot{u}_s^2(t)]/\dot{u}_m^2 + E[\ddot{u}_s^2(t)]/\ddot{u}_m^2 \}$$

where  $u_m$ ,  $\dot{u}_m$ ,  $\ddot{u}_m$  are the maximum mean square responses of displacement, velocity (stroke) and acceleration, respectively. The optimized mean square responses are plotted in Figures 10–12. In the figures, solid, triangular and dotted lines are for  $\mu=0$ , 0.05 and 0.1, respectively. One can obtain a similar conclusion as using displacement as cost function for a PSO optimization and we shall use displacement as the cost function in the following examples.

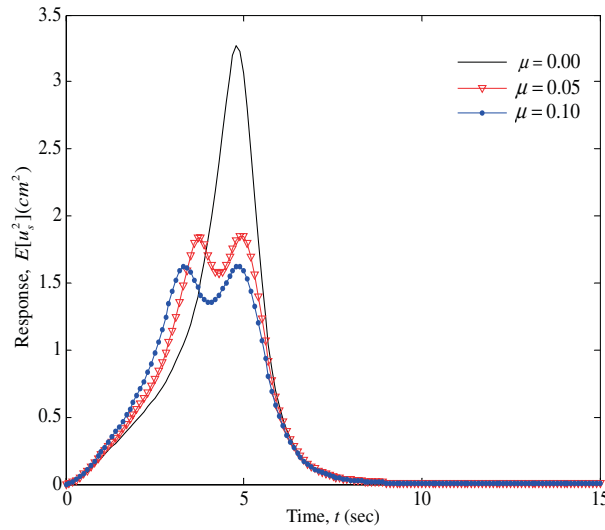


Figure 7. Displacement mean square responses using acceleration as the cost function.

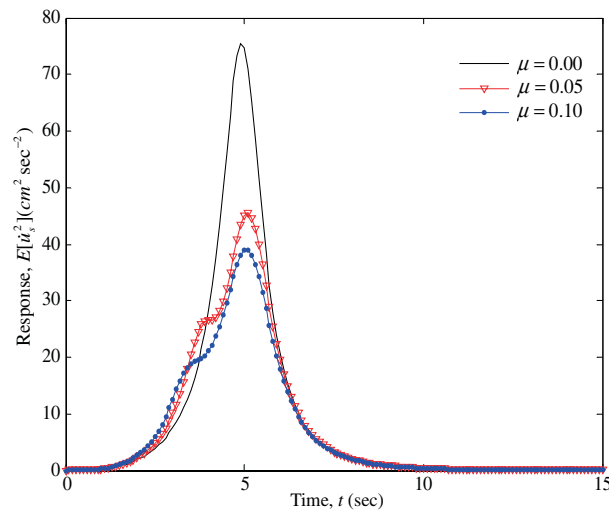


Figure 8. Velocity mean square responses using acceleration as the cost function.

The evolutionary mean square response of acceleration is large in the absolute value due to the fact that integrating

$$\frac{\omega_g^4 + 4\xi_g^2 \omega_g^2 \omega^2}{(\omega^2 - \omega_g^2)^2 + 4\xi_g^2 \omega_g^2 \omega^2} \times \omega^4$$

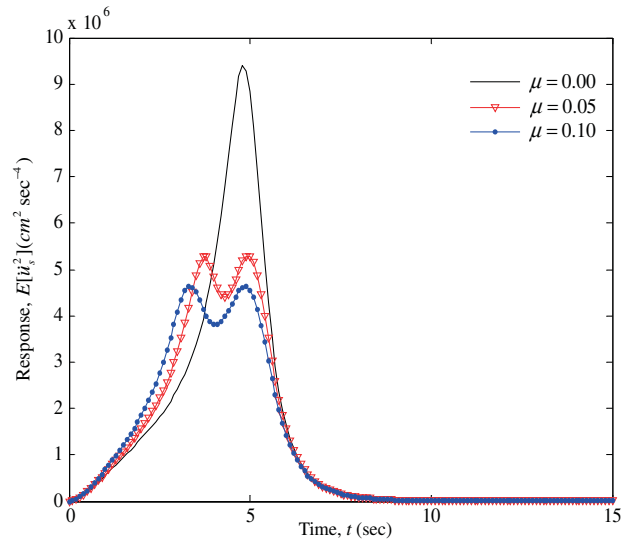


Figure 9. Acceleration mean square responses using acceleration as the cost function.

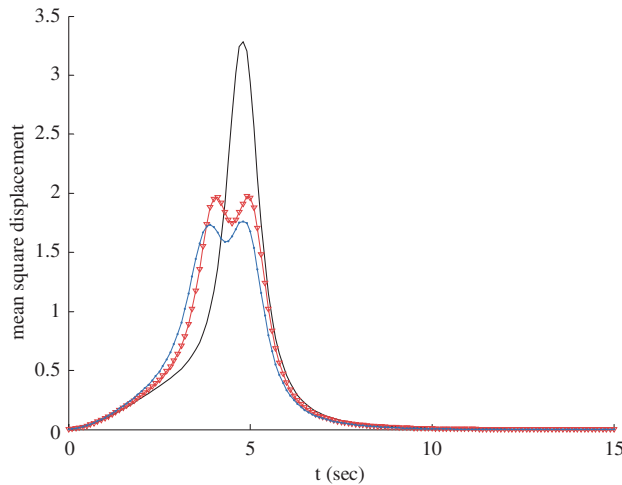


Figure 10. Displacement mean square responses.

over infinite frequency is unbound. It happens to all algorithms using Kanai-Tajimi spectrum. Here, we use the cut-off frequency at 200 rad/s in all calculations. In fact, the natural frequency is 5 rad/s and the peak excitation is  $\omega_g = 15.0$  rad/s. A cut-off frequency of 30 rad/s is sufficient. The calculated values are much reduced, but the response shapes do not change visibly. The percentage reduction at optimum is about the same.

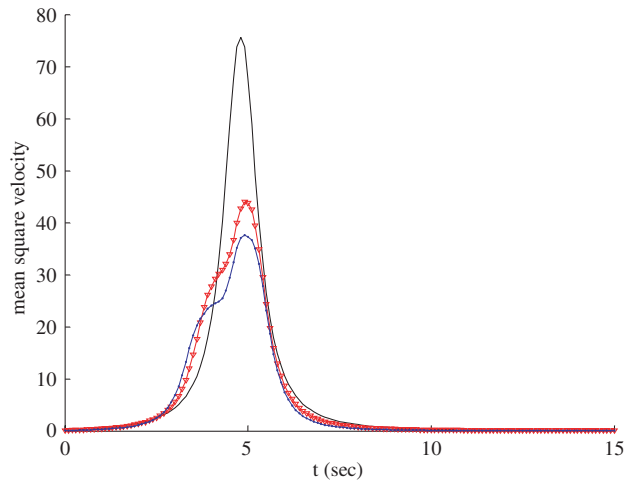


Figure 11. Velocity mean square responses.

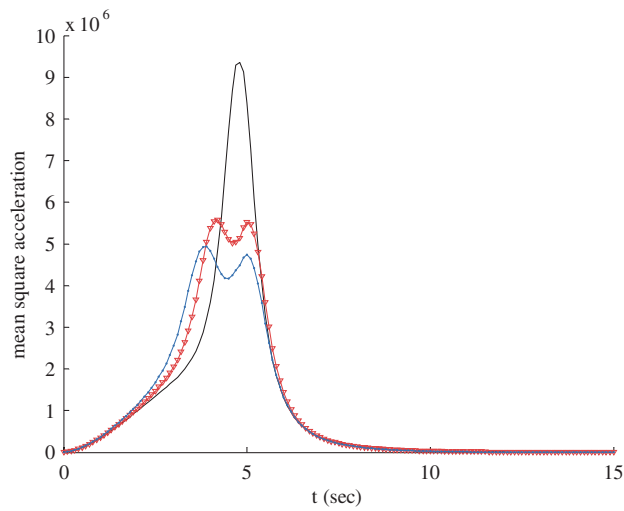


Figure 12. Acceleration mean square responses.

### *Power spectrum II*

The evolutionary power spectrum is to simulate the behavior of the E–W component of the December 30, 1934 EI Centro earthquake, and the analytic expression of the evolutionary spectrum

is as follows:

$$S\ddot{u}_g(\omega, t) = |\lambda(\omega, t)|^2 S_0 \tag{21}$$

$$\lambda(\omega, t) = \frac{e^{-at} - e^{-bt}}{\max[e^{-at} - e^{-bt}]} \left\{ \frac{\omega_{g1}^4 + 4\zeta_g^2 \omega_{g1}^2 \omega^2}{(\omega^2 - \omega_{g1}^2)^2 + 4\zeta_g^2 \omega_{g1}^2 \omega^2} \right\}^{1/2} + e^{-(t-l)^2/2\sigma^2} \left\{ \frac{\omega_{g2}^4 + 4\zeta_g^2 \omega_{g2}^2 \omega^2}{(\omega^2 - \omega_{g2}^2)^2 + 4\zeta_g^2 \omega_{g2}^2 \omega^2} \right\}^{1/2} \tag{22}$$

where  $a=0.25\text{ s}^{-1}$ ;  $b=0.50\text{ s}^{-1}$ ;  $\zeta_g=0.25$ ;  $\omega_{g1}=15.0\text{ rad/s}$ ;  $\omega_{g2}=30.0\text{ rad/s}$ ;  $l=5.0\text{ s}$ ;  $\sigma=1.0\text{ s}$ ; and  $S_0=2.0\text{ cm}^2/\text{s}^3$ . Similarly, the optimum parameters and the displacement mean square response quantities for specified mass ratio  $\mu$  are given in Table III after using PSO to optimize the damping  $\zeta_T$  and tuning frequency ratio  $f$ . The optimum damping and tuning frequency of TMD for the main system are plotted in Figures 13 and 14 as functions of mass ratio. From Figure 13, it is also seen that the optimum damping  $\zeta_T^{\text{opt}}$  increases with increasing mass

Table III. Optimum TMD parameters for the main system under non-stationary random ground acceleration with power spectrum II based on PSO for a specified mass ratio.

$\mu$	0.01	0.02	0.03	0.04	0.05	0.06	0.07	0.08	0.09	0.1
$\zeta_T^{\text{opt}}$	0.0000	0.0000	0.0127	0.0320	0.0401	0.0453	0.0593	0.0614	0.0718	0.0738
$f^{\text{opt}}$	0.9392	0.9164	0.9020	0.8925	0.8812	0.8689	0.8614	0.8503	0.8426	0.8329
$N^{\text{opt}} (\text{cm}^2)$	14.7397	12.2766	10.9056	9.9108	9.1251	8.5317	8.0390	7.6038	7.2594	6.9305

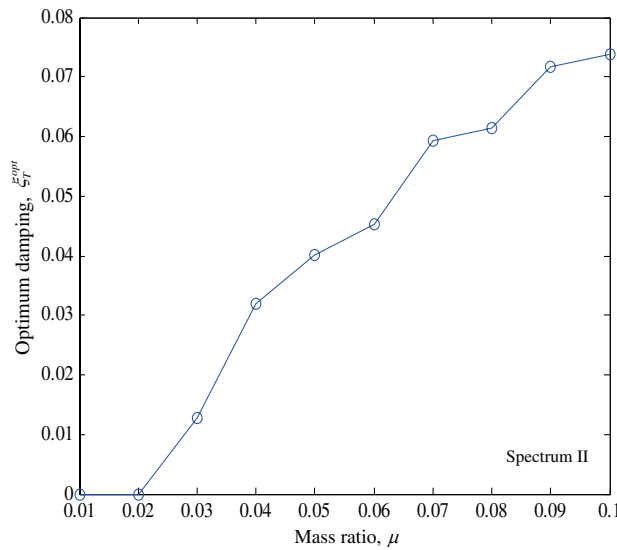


Figure 13. Optimum damping of a TMD for evolutionary spectrum II.



ratio  $\mu$ . From Figure 14, it is observed that the optimum tuning frequency  $f^{opt}$  always decreases with the increase in the mass ratio  $\mu$ .

Similarly, the variations of the displacement mean square responses and the corresponding velocity mean square responses for different specified mass ratios  $\mu$  are plotted in Figures 15–17, respectively. The system maximum responses further reduce with the increase in the mass of the optimum TMD. For the mass ratio  $\mu = 0.1$ , compared with the case of the main system without

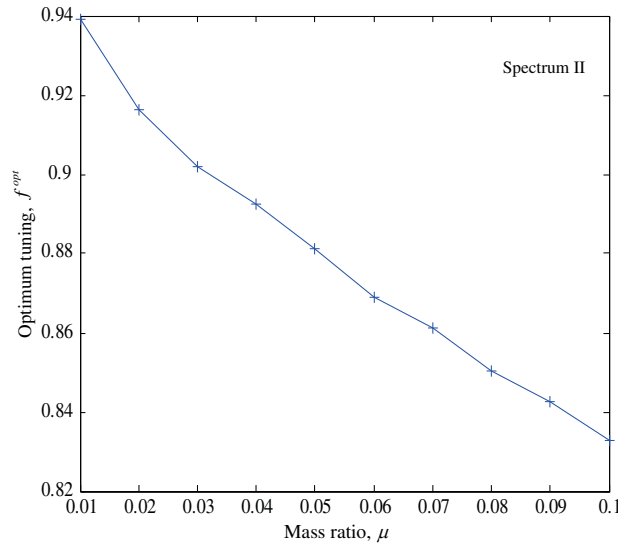


Figure 14. Optimum tuning frequency of a TMD for evolutionary spectrum II.

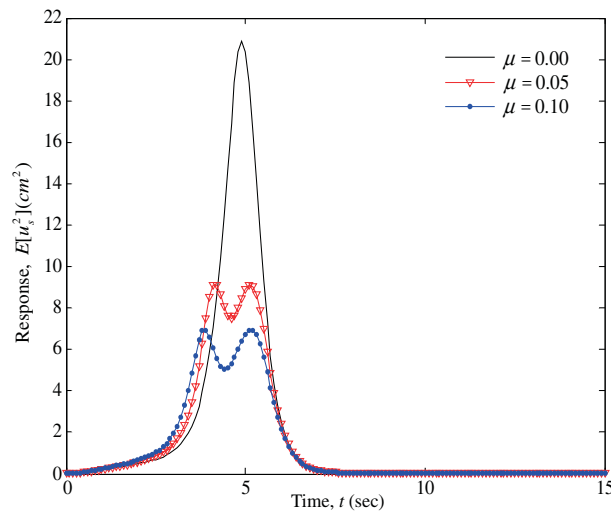


Figure 15. Displacement mean square responses of the main system for evolutionary spectrum II.

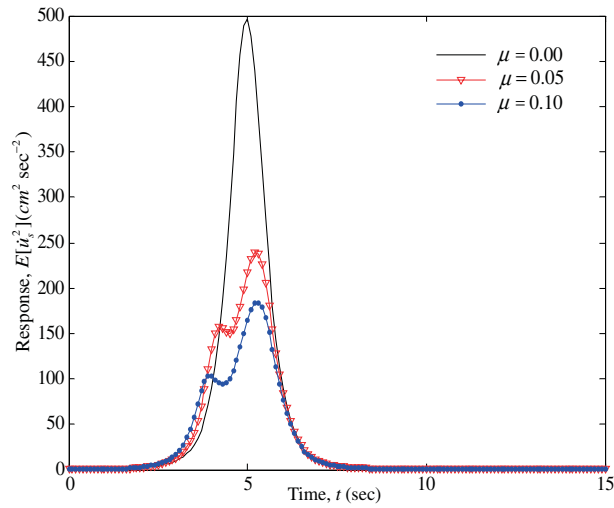


Figure 16. Corresponding velocity mean square responses of the main system for evolutionary spectrum II.

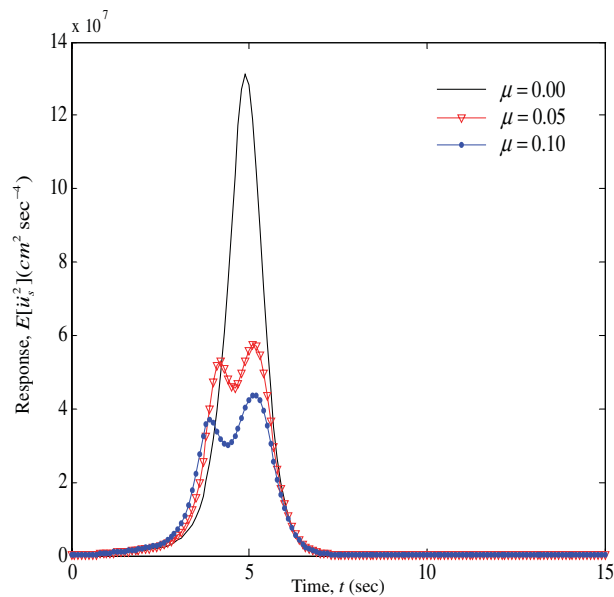


Figure 17. Acceleration mean square responses of the main system for evolutionary spectrum II.

a TMD, the maximum displacement mean square response  $E[u_s^2]$ , the maximum velocity mean square response  $E[\dot{u}_s^2]$  and the maximum acceleration mean square response  $E[\ddot{u}_s^2]$  of the main system are reduced by 66.81, 62.90 and 61.5%, respectively.

*Power spectrum III*

The evolutionary power spectrum is to simulate the acceleration record of the 1964 Niigata earthquake, and the evolutionary spectrum is expressed as

$$S_{\ddot{u}_g}(\omega, t) = |\lambda(\omega, t)|^2 S_0 \tag{23}$$

$$\lambda(\omega, t) = \frac{e^{-at} - e^{-bt}}{\max[e^{-at} - e^{-bt}]} \left\{ \frac{\omega_g^4(t) + 4\xi_g^2(t)\omega_g^2(t)\omega^2}{[\omega^2 - \omega_g^2(t)]^2 + 4\xi_g^2(t)\omega_g^2(t)\omega^2} \right\}^{1/2} \tag{24}$$

where the constants  $a$ ,  $b$  and  $S_0$  have the same values as those described in Sections 4.1 and 4.2. At the same time, the functions  $\xi_g(t)$  and  $\omega_g(t)$ , respectively, are defined as follows:

$$\xi_g(t) = \begin{cases} 0.64 & (0 \leq t < 4.5 \text{ s}) \\ 1.25(t - 4.5)^3 - 1.875(t - 4.5)^2 + 0.64 & (4.5 \text{ s} \leq t < 5.5 \text{ s}) \\ 0.015 & (5.5 \text{ s} \leq t) \end{cases} \tag{25}$$

$$\omega_g(t) = \begin{cases} 15.56 & (0 \leq t < 4.5 \text{ s}) \\ 27.12(t - 4.5)^3 - 40.68(t - 4.5)^2 + 15.56 & (4.5 \text{ s} \leq t < 5.5 \text{ s}) \\ 2.0 & (5.5 \text{ s} \leq t) \end{cases} \tag{26}$$

Similarly, using PSO to optimize the damping  $\xi_T$  and tuning frequency ratio  $f$  of the TMD for a specified mass ratio  $\mu$ , the optimum results for a specified mass ratio  $\mu$  are given in Table IV. The optimum damping and tuning frequency of the TMD for the main system are shown in Figures 18 and 19 as functions of mass ratio. From Figure 18, it is seen that the optimum damping  $\xi_T^{\text{opt}}$  increases as the mass ratio  $\mu$  increases as well. From Figure 19, it is observed that the optimum tuning frequency  $f^{\text{opt}}$  decreases more slowly than that of the case for evolutionary power spectrum I with the increase in the mass ratio  $\mu$ .

Similarly, the variations of the displacement mean square responses and the corresponding velocity and acceleration mean square responses for different specified mass ratios  $\mu$  are shown in Figures 20–22, respectively, which demonstrates that the system maximum responses further reduce with the increase in the mass of the optimum TMD. Comparing with the main system without a TMD for the mass ratio  $\mu=0.1$ , the maximum displacement mean square response  $E[u_s^2]$  and the maximum velocity mean square response  $E[\dot{u}_s^2]$  of the main system are reduced by 48.48 and 48.53%, respectively. The sudden drop in the acceleration mean square response shown in Figure 22 at 5 s is due mainly to the merging of two peaks in the displacement and velocity diagrams into one peak.

Table IV. Optimum TMD parameters for the main system under non-stationary random ground acceleration with power spectrum III based on PSO for a specified mass ratio.

$\mu$	0.01	0.02	0.03	0.04	0.05	0.06	0.07	0.08	0.09	0.1
$\xi_T^{\text{opt}}$	0.0000	0.0187	0.0337	0.0511	0.0687	0.0831	0.0936	0.1098	0.1205	0.1307
$f^{\text{opt}}$	0.8640	0.8278	0.7996	0.7800	0.7628	0.7457	0.7274	0.7144	0.7000	0.6869
$N^{\text{opt}}$ (cm <sup>2</sup> )	1.8190	1.6200	1.5179	1.4452	1.3957	1.3578	1.3284	1.3051	1.2831	1.2626

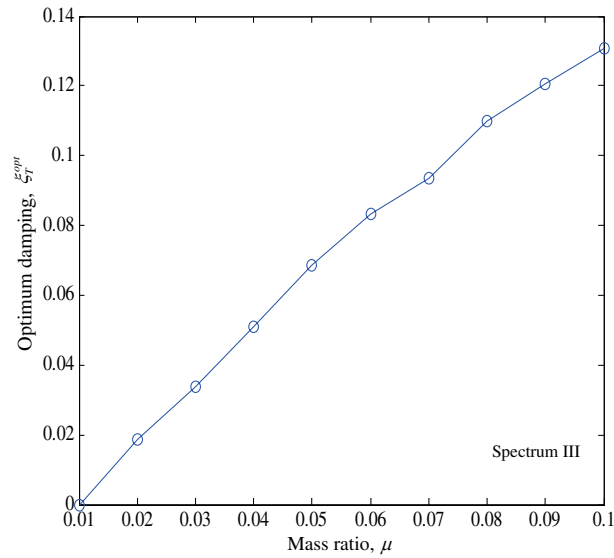


Figure 18. Optimum damping of the TMD for evolutionary spectrum III.

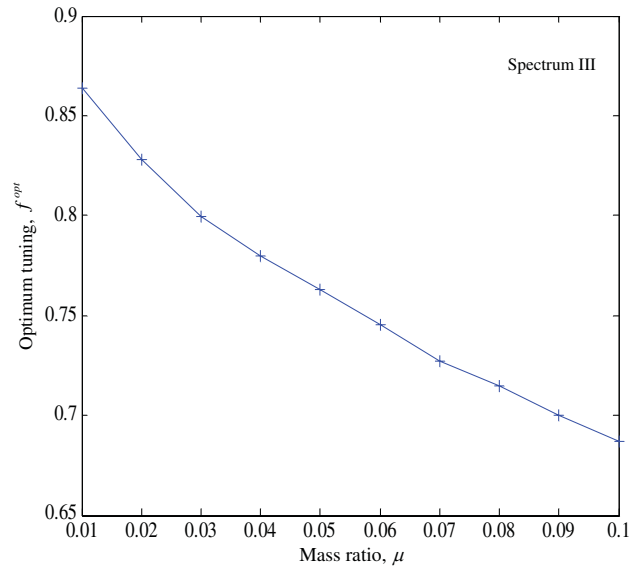


Figure 19. Optimum tuning frequency of the TMD for evolutionary spectrum III.

In addition, from Tables I to IV, we note that the impact of the damping of TMD on the responses of the main system is becoming negligible along with the decrease in the mass ratio (i.e. mass ratio  $\mu \leq 0.01$ ).

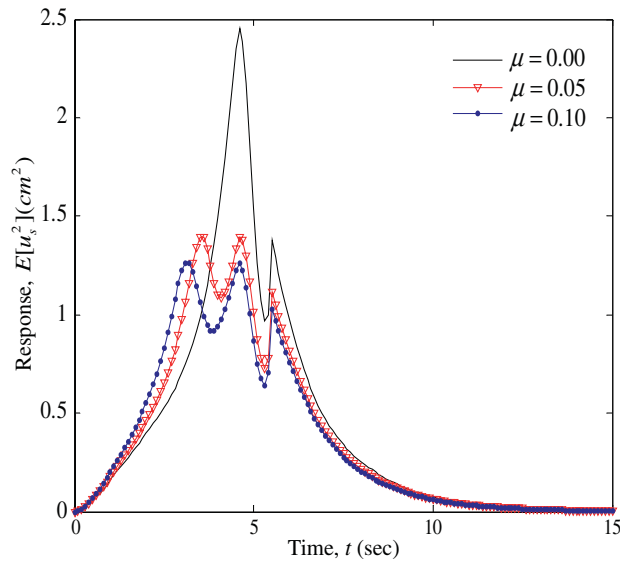


Figure 20. Optimum displacement mean square responses of the main system for evolutionary spectrum II.

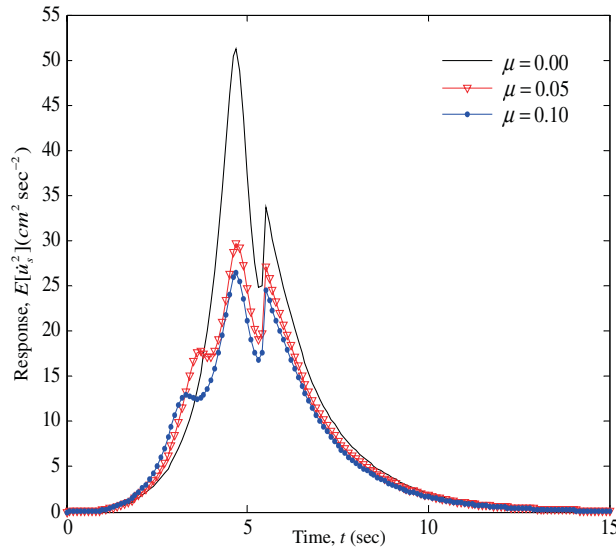


Figure 21. Corresponding velocity mean square responses of the main system for evolutionary spectrum II.

*Analysis of computing accuracy*

PSO algorithm is a numerical method to optimize TMD parameters under non-stationary base excitations. The computing errors are mainly caused by two aspects.

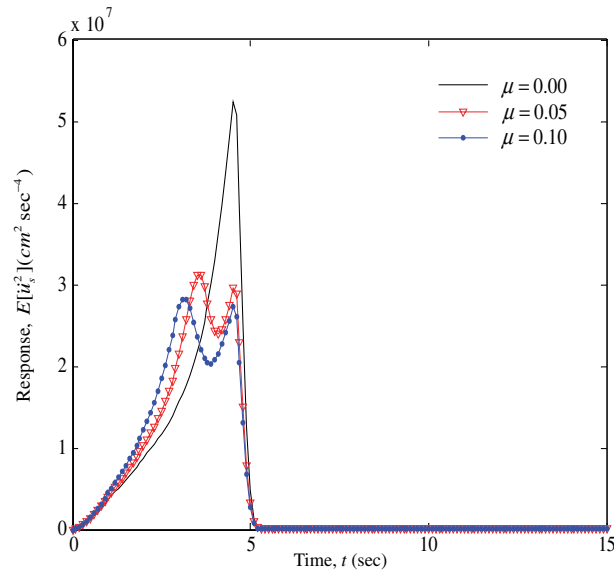


Figure 22. Mean square of acceleration response.

On the one hand, the computing errors are from cost function calculation. For this part, the integration step size of natural frequency  $\Delta\omega$ , the integration step size of time series  $\Delta t$  and the calculation step size in the Runge–Kutta integration method influence the calculation accuracy. Reference [17] has proved that the accuracy is high enough by comprising with other analytical methods.

On the other hand, the parameters of PSO such as the population size of particles and numbers of iteration may also have an impact on the optimization results. According to this, after a lot of testing, we discover that the optimum solutions are not sensitive to the changes in the population for power spectrum I, II and III. Certainly, there is no doubt that PSO converges faster to the optimum results if the population is increased. In contrast, due to the complexity of the issues, the maximum generation influences the optimization results to some extent. We can increase it to obtain the better results so as to meet engineering requirements.

## CONCLUSIONS

To the best of our knowledge, this is the first report on the application of particle swarm optimization (PSO) to TMD optimization issues for non-stationary random excitation applied to a damped main system. The optimum TMD parameters for the damped SDOF main system subjected to ground accelerations with different evolutionary power spectra are obtained by using PSO for the minimization of either the maximum displacement or acceleration mean square responses. The variation of optimum parameters and displacement and velocity mean square responses as functions of time series are also analyzed from optimization results, which demonstrates the performance and efficiency of PSO. It is quite easy to be programmed for applications of PSO in practical engineering.

Although the results in the present study are calculated numerically, it will guarantee the accuracy for engineering applications as long as the integration step-size is small enough and the maximum generation is large enough. The future work is to focus on using new computing techniques instead of the Runge–Kutta integration method for the sake of time saving. At the same time, the applications of multi-objectives PSO simultaneously considering the minimization of displacement and velocity responses of the main systems equipped with a TMD under non-stationary random excitations will be promising.

## ACKNOWLEDGEMENTS

This research is supported by CERG#115706 of the Research Grant Council of Hong Kong awarded to Professor A. Y. T. Leung.

## REFERENCES

1. Rana R, Soong TT. Parametric study and simplified design of tuned mass dampers. *Engineering Structures* 1998; **20**:193–204.
2. Lee CL, Chen YT, Chung LL, Wang YP. Optimal design theories and applications of tuned mass dampers. *Engineering Structures* 2006; **28**(1):43–53.
3. Den Hartog JP. *Mechanical Vibrations* (4th edn). McGraw-Hill: New York, 1956.
4. Brock JE. A note on the damped vibration absorber. *Journal of Applied Mechanics* (ASME) 1946; **13**(4):A-284.
5. Warburton GB, Ayorinde EO. Optimum absorber parameters for simple systems. *Earthquake Engineering and Structural Dynamics* 1980; **8**:197–217.
6. Ayorinde EO, Warburton GB. Minimizing structural vibrations with absorbers. *Earthquake Engineering and Structural Dynamics* 1980; **8**:219–236.
7. Warburton GB. Optimum absorber parameters for minimizing vibration response. *Earthquake Engineering and Structural Dynamics* 1981; **9**:251–262.
8. Warburton GB. Optimum absorber parameters for various combinations of response and excitation parameters. *Earthquake Engineering and Structural Dynamics* 1982; **10**:381–401.
9. Bapat VA, Kumaraswamy HV. Effect of primary system damping on the optimum design of an untuned viscous dynamic vibration absorber. *Journal of Sound and Vibration* 1979; **63**:469–474.
10. Thompson AG. Optimizing the untuned viscous dynamic vibration absorber with primary system damping: a frequency locus method. *Journal of Sound and Vibration* 1980; **73**:469–472.
11. Tsai H-C, Lin G-C. Optimum tuned-mass dampers for minimizing steady-state response of support-excited and damped systems. *Earthquake Engineering and Structural Dynamics* 1993; **22**:957–973.
12. Tsai H-C, Lin G-C. Explicit formulae for optimum absorber parameters for force-excited and viscously damped system. *Journal of Sound and Vibration* 1994; **176**:585–596.
13. Jangid RS. Optimum multiple tuned mass dampers for base-excited undamped system. *Earthquake Engineering and Structural Dynamics* 1999; **28**:1041–1049.
14. Bakre SV, Jangid RS. Optimum parameters of tuned mass damper for damped main system. *Structural Control and Health Monitoring* 2007; **14**:448–470.
15. Bakre SV, Jangid RS. Optimum multiple tuned mass dampers for base-excited damped main system. *International Journal of Structural Stability and Dynamics* 2004; **4**:527–542.
16. Jangid RS. Response of SDOF system to non-stationary earthquake excitation. *Earthquake Engineering and Structural Dynamics* 2004; **33**:1417–1428.
17. Li J. Calculation for evolutionary random seismic response of building structures with TMD. *Building Structure* 2005; **35**:21–23, 27 (in Chinese).
18. Kennedy J, Eberhart RC. Particle swarm optimization. *Proceedings of the IEEE International Conference on Neural Networks (ICNN'95)*, Perth, Australia, November/December 1995; 1942–1948.
19. Shi Y, Eberhart RC. A modified swarm optimizer. *IEEE International Conference of Evolutionary Computation*. IEEE Press: Anchorage, Alaska, 1998; 69–74.
20. Kennedy J, Eberhart RC, Shi Y. *Swarm Intelligence*. Morgan Kaufmann: San Francisco, CA, 2001.

21. He Q, Wang L. An effective co-evolutionary particle swarm optimization for constrained engineering design problems. *Engineering Application of Artificial Intelligence* 2007; **20**:89–99.
22. De Falco I, Della Cioppa A, Tarantino E. Facing classification problems with particle swarm optimization. *Applied Soft Computing* 2007; **7**:652–658.
23. Saidi H, Khelil N, Hassouni S *et al.* Energy spectra of the Schrodinger equation and the differential quadrature method: improvement of the solution using particle swarm optimization. *Applied Mathematics and Computation* 2006; **182**:559–566.
24. Cui SM, Weile DS. Application of a parallel particle swarm optimization scheme to the design of electromagnetic absorbers. *IEEE Transactions on Antennas and Propagation* 2005; **53**:3616–3624.
25. Lu WZ, Fan HY, Leung AYT, Wong JCK. Analysis of pollutant levels in central Hong Kong applying neural network method with particle swarm optimization. *Environmental Monitoring and Assessment* 2002; **79**(3): 1995–2012.
26. Deodatis G, Shinozuka M. Auto-regressive model for non-stationary stochastic process. *Journal of Engineering Mechanics* 1988; **114**:1995–2012.
27. Fang T, Li J, Sun M. A universal solution for evolutionary random response problems. *Journal of Sound and Vibration* 2002; **253**:909–916.